

# Interaction between Surface Acoustic Wave and Quantum Hall Effects

Xiao Liu,<sup>1</sup> Mengmeng Wu,<sup>1</sup> Renfei Wang,<sup>1</sup> Xinghao Wang,<sup>1</sup> Wenfeng Zhang,<sup>1</sup> Yujiang Dong,<sup>1</sup> Rui-Rui Du,<sup>1,2</sup> Yang Liu,<sup>1,3,\*</sup> and Xi Lin<sup>1,3,4,†</sup>

<sup>1</sup>International Center for Quantum Materials, Peking University, Beijing, China, 100871  
<sup>2</sup>Center for Excellence, University of Chinese Academy of Sciences, Beijing, China, 100190  
<sup>3</sup>Hefei National Laboratory, Hefei, China, 230088

<sup>4</sup>Interdisciplinary Institute of Light-Element Quantum Materials and Research Center for Light-Element Advanced Materials, Peking University, Beijing, China, 100871

(Dated: April 9, 2024)

Surface acoustic wave (SAW) is a powerful technique for investigating quantum phases appearing in two-dimensional electron systems. The electrons respond to the piezoelectric field of SAW through screening, attenuating its amplitude, and shifting its velocity, which is described by the relaxation model. In this work, we systematically study this interaction using orders of magnitude lower SAW amplitude than those in previous studies. At high magnetic fields, when electrons form highly correlated states such as the quantum Hall effect, we observe an anomalously large attenuation of SAW, while the acoustic speed remains considerably high, inconsistent with the conventional relaxation model. This anomaly exists only when the SAW power is sufficiently low.

## 1. INTRODUCTION

Research on charge carrier transport in two-dimensional electron systems (2DES) has unveiled various intriguing quantum phenomena [1–3]. The quantum Hall effect (QHE) is of interest due to its distinctive experimental phenomena: the vanishing of longitudinal resistivity and the precise quantization of Hall resistivity into discrete integers [1] and fractions [2]. Theoretical explanations for the QHE include the formation of an incompressible quantum liquid that carries superflow current, and disorder-induced localization of sparse quasiparticles[4] At sufficiently large perpendicular magnetic fields, when only several Landau level are occupied, and in samples with sufficiently high mobility, the Coulomb interaction arranges the sparse quasiparticles into an ordered array named the Wigner crystal [5–10]. Additionally, the stripe and bubble phases represent two other types of electron solids, emerging as collective charge density waves in the  $N \geq 1$  spin-resolved Landau levels  $N \geq 1$  spin-resolved Landau levels[11–13]. The interaction between these states and external perturbations, such as microwaves[14–19], acoustic waves[20–32], light[33], in-plane magnetic fields[34–38], bias voltage[39], noise[40] and hydrostatic pressure[41–43], presents avenues for exploring exotic physics and gaining profound insights into state evolution.

Surface acoustic wave (SAW) provides a contactless approach for investigating the transport properties of 2DES. As SAW propagates on the surface of GaAs/AlGaAs samples which are piezoelectric, its co-propagating piezoelectric field interacts with the adjacent 2DES through a relaxation process [44, 45]. This piezoelectric field will be fully screened when the electronic relaxation time (i.e. the transport lift time  $\tau_{tr}$ ) is shorter than the acoustic wave period. In the weak-coupling limit, the relaxation model predicts that the

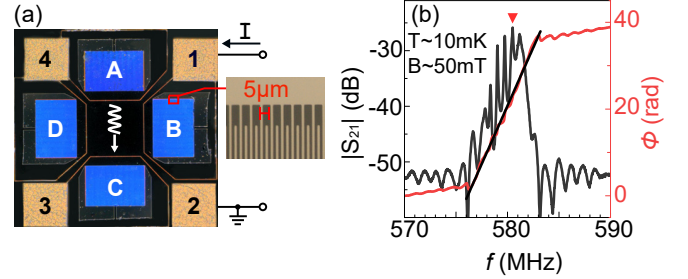


FIG. 1. (a) The image of our sample. The  $d_m = 1.2$ mm square van der Pauw mesa with four contacts is defined by wet etching. (b) The frequency spectrum measured by IDT pair A & C. The red triangle marks the resonance frequency  $f_c \approx 580.5$  MHz, at which all the rest measurements are performed.

SAW attenuation coefficient  $\Gamma$  and its normalized velocity shift  $\eta = \Delta v/v_0$  is related with the 2DES conductivity  $\sigma_{xx}$  as:

$$\Gamma = k \frac{K_{\text{eff}}^2}{2} \frac{\sigma_{xx}/\sigma_M}{1 + (\sigma_{xx}/\sigma_M)^2} \quad (1)$$

$$\eta = \Delta v/v_0 = \frac{K_{\text{eff}}^2}{2} \frac{1}{1 + (\sigma_{xx}/\sigma_M)^2} \quad (2)$$

where  $v_0 = v(\sigma_{xx} \rightarrow \infty)$  and  $K_{\text{eff}}^2$  is the effective piezoelectric coupling constant. The characteristic conductivity  $\sigma_M = v_0(\epsilon) \approx 4 - 7 \times 10^{-7} \Omega^{-1}$ , with  $\epsilon$  being the effective dielectric constant.

This relaxation model has been widely used to interpret experimental observations in many previous studies, where the SAW amplitude is large (namely many electrons are confined by the piezo-potential) [20–25, 29–31]. However, recent experimental observations suggest some insufficiencies when strongly correlated electron solid phases are present [26–28, 32]. In this work, we study 2DES using SAW amplitude that is orders of magnitude smaller than previous studies. Our data demon-

strate the inadequacy of the relaxation model at low filling factors. We find that the interaction between 2DES and SAW is influenced by the presence of current and changing acoustic power, which are also missed in the relaxation model.

## 2. SAMPLE AND METHODS

Our sample is fabricated from a GaAs/AlGaAs single-interface heterostructure grown by molecular-beam epitaxy whose 2DES layer is located approximately 120 nm below the surface. The electron density is  $1.12 \times 10^{11} \text{ cm}^{-2}$  and the low temperature mobility is  $\mu \sim 1 \times 10^6 \text{ cm}^2 \text{ V}^{-1} \text{ s}^{-1}$ . The 2DES mesa is a  $1.2 \times 1.2 \text{ mm}^2$  square at the center, with four annealed Ge/Au/Ni/Au Ohmic contacts at the corners of the sample. Four interdigital transducers (IDTs), fabricated using maskless laser lithography, are symmetrically arranged around the square mesa. Each IDT consists of 170 pairs of  $1 \mu\text{m}$  wide Al finger electrodes, separated by an interdigitated gap of  $1.5 \mu\text{m}$ . Such IDT configuration generates SAW with a wavelength of  $\lambda = 5 \mu\text{m}$  if excited at its resonance frequency  $f_c = 580.5 \text{ MHz}$ ; see Fig.1(b). The aperture of the IDT spans  $1220 \mu\text{m}$ , slightly wider than the mesa. We removed 200-nm-thick AlGaAs below the IDT, including all doping layers, to ensure optimal performance. All the measurements are conducted in a dilution refrigerator whose base temperature is approximately 10 mK.

The frequency dependence of the amplitude and phase of the transmission coefficient,  $|\mathbf{S}_{21}|$  and  $\phi$ , is illustrated in Fig.1(b). The data is measured at 50 mT and fridge base temperature. The low-field SAW velocity can be estimated from the resonance frequency through  $v_0 = f_c \cdot \lambda \simeq 2900 \text{ m/s}$ , and its total traveling time can be deduced from the phase-frequency relation within the resonance peak  $\tau_0 = \partial\phi/\partial(2\pi f) = 0.85 \mu\text{s}$ . This estimated SAW travel distance  $d = v_0\tau_0 \simeq 2.5 \text{ mm}$  is consistent with the  $2450 \mu\text{m}$  center-to-center distance between opposite IDTs. A homemade RF lock-in amplifier with high sensitivity and low noise was utilized to monitor the amplitude and phase shift [46]. The SAW velocity shift is calculated as  $\eta = \phi/2\pi f_c \tau$ , with  $\tau \simeq 0.4 \mu\text{s}$ , the SAW traveling time through the  $1.2 \text{ mm}$  square 2DES mesa [32]. Unless otherwise specified, the input excitation power applied to the IDT is 1 nW.

## 3. RESULTS AND DISCUSSION

Figure 2(a-c) show the longitudinal magneto-resistance  $R_{xx}$  measured using conventional lock-in techniques at 7.3 Hz, the SAW attenuation coefficient  $\Gamma$  and velocity shift  $\eta$  in reference with their zero magnetic field values. By comparing Fig. 2(a) and (c) data, the SAW results are more reliable and sensitive than the conventional transport

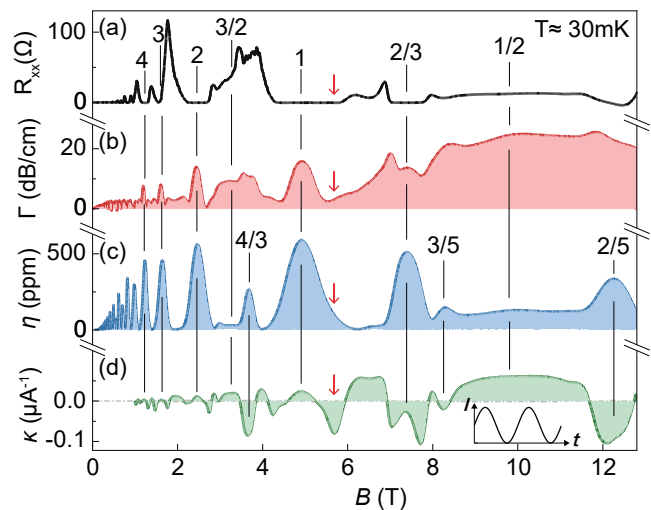


FIG. 2. (a-c) The longitudinal resistance  $R_{xx}$  measured using conventional 4-point transport measurement, the SAW attenuation coefficient  $\Gamma$  and velocity shift  $\eta$  measured when all contacts are grounded. (d) The current induced SAW velocity shift measured when an oscillating positive current (see the inset) flows between contacts 1 and 2.

measurement. For example, features corresponding to the  $\nu = 4/3$  fractional quantum Hall effect are clearly seen in Fig. 2(c) while they are invisible in Fig. 2(a). Although the response of other phases such as CDW in SAW measurement is not well understood, the observed  $\nu = 4/3$  feature is more likely a signature of quantum Hall liquid. This is because the formation of CDW phases can either cause anisotropic  $\eta$  or a negative  $\eta$ [26] which is not the case here. SAW measurement exhibits features even if droplets of quantum Hall liquid appear, while showing transport features requires the quantum Hall region be sufficiently large to conduct the dissipation-less current. The better performance of SAW measurement can also be seen at low magnetic fields, illustrated in Fig. 3(a). The conductivity of 2DES exhibits Shubnikov-de Haas (SdH) oscillations, and the oscillation in  $\eta$  starts at similar field as the best  $R_{xx}$ . Enhanced  $\eta$ , seen as maximum in Fig. 2(c), appears at even integer filling factors when the magnetic field exceeds about 0.1 T. Above 0.38 T, maximum develops at odd integer fillings, corresponding to the breaking of spin degeneracy. This is also similar to the  $R_{xx}$  data. The fact that acoustic speed increases at integer fillings is consistent with the relaxation model, where the 2DES's screening capability against piezoelectric fields vanishes when it forms an incompressible quantum Hall liquid. The electrons become mobile when the 2DES is compressible at half-integer fillings. They screen the SAW's piezoelectric fields and slow down the sound velocity. It is quite surprising that  $\eta$  almost always equals its zero-field value, despite the fact that the conductivity of 2DES in these high mobility samples vanishes as

$B^{-2}$  [47].

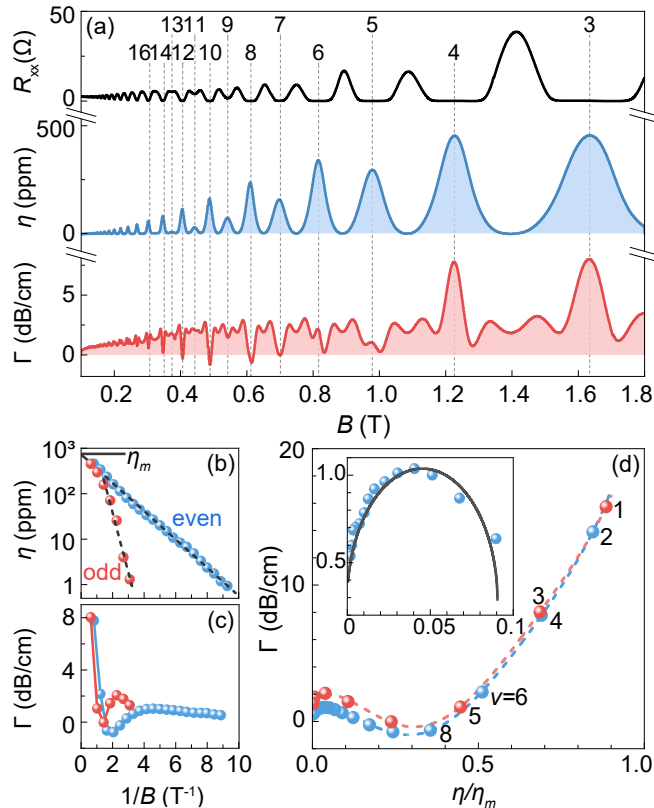


FIG. 3. (a) Expanded plot of  $\eta$  and  $\Gamma$  at low magnetic field. (b)  $\eta$  vs.  $1/B$  exhibits an exponential relation for both even and odd integer filling factors. The red/blue dots are experiment data at odd/even fillings. The black dashed lines are the fitting curves, see text. (c)  $\Gamma$  vs.  $1/B$ . (d) The relation between  $\Gamma$  and the normalized velocity shift  $\eta/\eta_m$ . The inset displays the high filling factors datapoints and the black line is the best fitting with Eqs.(1) and (2) using  $K_{\text{eff}}^2 = 1.2 \times 10^{-4}$ .

We now summarize the  $\eta$  and  $\Gamma$  at integer fillings as a function of their corresponding magnetic fields in Fig. 3(b-c). We find that  $\eta$  has a clear exponential dependence on  $1/B$  over nearly 3 orders of magnitude. Note that the relaxation model is not suitable to describe the interaction between the SAW and the incompressible QHE when the screening is likely caused by creating quasiparticles/quasiholes. One would not be surprised to see the exponential relation  $\eta \propto \exp(-\Delta_e/\hbar\omega_c)$  and  $\eta \propto \exp(-\Delta_o/E_Z)$  at odd and even filling factors, respectively. By fitting the data in Fig. 3(b), we can deduce the energy that describes this SAW-2DES interaction,  $\Delta_e \simeq 14\text{K}$  and  $\Delta_o \simeq 0.9\text{K}$ . Here,  $\hbar\omega_c$  is the cyclotron energy and  $E_Z$  is the Zeeman energy.

The deviation of our experimental results with the relaxation model is more pronounced in the evolution of the SAW attenuation  $\Gamma$ . When we increase the magnetic field,  $\Gamma$  at integer fillings first increases and reaches its maximum at about 0.2 T before decreasing. This is

expected by the relaxation model and the  $\Gamma$  maximum signals that  $\sigma_{xx} = \sigma_M$ . When we further increase the magnetic fields to above 0.8 T, a peak in  $\Gamma$  appears at integer fillings in contrast to the  $\Gamma$  minimum seen at low fields. This peak becomes dominant at the filling factor  $\nu = 4$  and continuously grows larger as we decrease the filling factor.

The anomalously increasing  $\Gamma$  after the low-field peak, seen when  $\sigma_{xx} = \sigma_M$ , while  $\eta$  monotonically increases, is counterintuitive. The 2DES becomes more incompressible and the SAW-2DES interaction should be even weaker for QHE at lower fillings. Furthermore,  $\Gamma$  seen at low fillings is much larger than its low field values in all conditions (below 3 dB/cm in Fig. 3(a)). We also note that at  $\nu = 1/2, 3/2$ , where the 2DES is compressible and  $\eta$  equals its zero field value,  $\Gamma$  becomes an order of magnitude larger than its low field values; note that the unit of  $\Gamma$  is logarithmic in Fig. 3. A possible reason could be attributed to the emergence of correlated states stabilized by the strong electron-electron interactions at low filling factors, such as quantum Hall effects, composite fermion Fermi sea, Wigner crystals, etc. These states might be effective in damping the SAW's piezoelectric fields by mechanisms such as electron-electron scattering, while their long range correlation prevents the reducing of the acoustic velocity.

We summarize the  $\eta$  and  $\Gamma$  values for even and odd integer filling factors and depicted in Fig. 3(d). The  $\Gamma$  vs. the normalized velocity shift  $\eta/\eta_m$  relation is almost the same for the odd and even filling factors. Here,  $\eta_m \simeq 663$  ppm is the maximum SAW velocity shift at  $1/B = 0$  T<sup>-1</sup> obtained from fitting the Fig. 3(b) data. The relaxation model is only applicable to high filling factor states, see the Fig. 3(d) inset. At low filling factors,  $\Gamma$  increases nearly linearly with  $\eta$ , and we do not observe any sign of saturation in  $\Gamma$  up to  $\nu = 1$ . As far as we know, a suitable theoretical modeling of the SAW-2DES interaction is missing. We hope that our clear experimental observations can help to stimulate future investigations.

We would like to emphasize that the above observations can only be seen when using extremely low SAW powers, and the presence of a conducting current can also vary the observed  $\Gamma$  and  $\eta$  [48]. In Fig. 4(c-d), we measured the variations in attenuation coefficient ( $\delta\Gamma = \Gamma(I) - \Gamma(0)$ ) and velocity shift ( $\delta\eta = \eta(I) - \eta(0)$ ) as a function of DC current  $I_{\text{DC}}$  at  $\nu = 1$  with various input SAW powers. The variations of  $\Gamma$  and  $\eta$  with SAW power when  $I_{\text{DC}} = 0$  are depicted in Fig. 4 (a & b).

At  $\nu = 1$ ,  $\Gamma$  decreases by about 15 dB/cm when increasing the SAW power from 1 nW to about 80 nW. This is to say, the anomalous  $\Gamma$  peak seen in Fig. 2(b) can only be seen at sufficiently low SAW amplitude. On the other hand,  $\Gamma$  slightly increases by about 2 dB/cm when we increase the current to almost 1  $\mu\text{A}$ . Meanwhile, increasing SAW amplitude reduces  $\eta$ , while DC current

leads to an increasing  $\eta$ . This is rather interesting as the data suggests that SAW and current have opposite effect on the 2DES. One other noteworthy feature in Fig. 4(c) and (d) are the fact that the current effect has a clear threshold of about 300 nA in the 1 nW SAW power trace, which disappears at large SAW power.

In order to compare the DC current effect for different phases, we applied a 0.25 Hz, 400 nA peak-to-peak AC current with a 200 nA DC offset between contacts 1 and 2 of the sample. The resulting change in SAW velocity is represented by a normalization parameter  $\kappa = \eta_m^{-1} \cdot (\partial\eta/\partial|I|)$ .  $\kappa$  approaches zero when the QHE is strong, e.g. at integer  $\nu = 1, 2, 3$ , etc. or fractional  $\nu = 2/3$ . This is expected from the threshold feature seen in Fig. 4(b). On the other hand, when the QHE is fragile at  $\nu = 4/3, 2/5$ , a substantial negative  $\kappa$  is observed, suggesting that the applied current makes the 2DES more efficient in slowing down the acoustic wave.

In Fig. 2(d),  $\kappa$  has a large negative value on the edge of the  $R_{xx}$  plateaus. In Fig. 4(a-b & e-f), we focus on one of these negative  $\kappa$  peaks at 5.7 T (marked by arrows in Fig.2). As we have discussed earlier, increasing SAW power and sending current have opposite effect on  $\eta$  and  $\Gamma$  at  $\nu = 1$ , they lead to qualitatively the same outcome at 5.7 T. In both cases,  $\eta$  decreases and  $\Gamma$  increases. We note that, the  $\Lambda$ -shape maximum of the  $\eta$  vs.  $I_{DC}$  relation at low SAW power becomes flat at large SAW power, opposite to the observed trend at  $\nu = 1$ . We also would like to point out that the changes in  $\eta$  and  $\Gamma$  tend to saturate at  $I_{DC} \gtrsim 700$  nA, while no sign of saturation is seen at  $\nu = 1$  until 2  $\mu$ A, which is still far less than the breakdown current of the  $\nu = 1$  QHE.

#### 4. CONCLUSION

Our systematic study shows that the conventional relaxation model is insufficient in describing the SAW-2DES interaction at very low SAW power and when 2DES forms strongly correlated states. We present as much experimental evidence as possible, and hope a comprehensive theoretical models can be proposed in the future.

#### ACKNOWLEDGMENTS

We acknowledge support by the National Key Research and Development Program of China (Grant No. 2021YFA1401900 and 2019YFA0308403), the Strategic Priority Research Program of the Chinese Academy of Sciences (Grant No. XDB33030000), the National Natural Science Foundation of China (Grant No. 92065104, 12074010 and 12141001) and the Innovation Program for Quantum Science and Technology (Grant

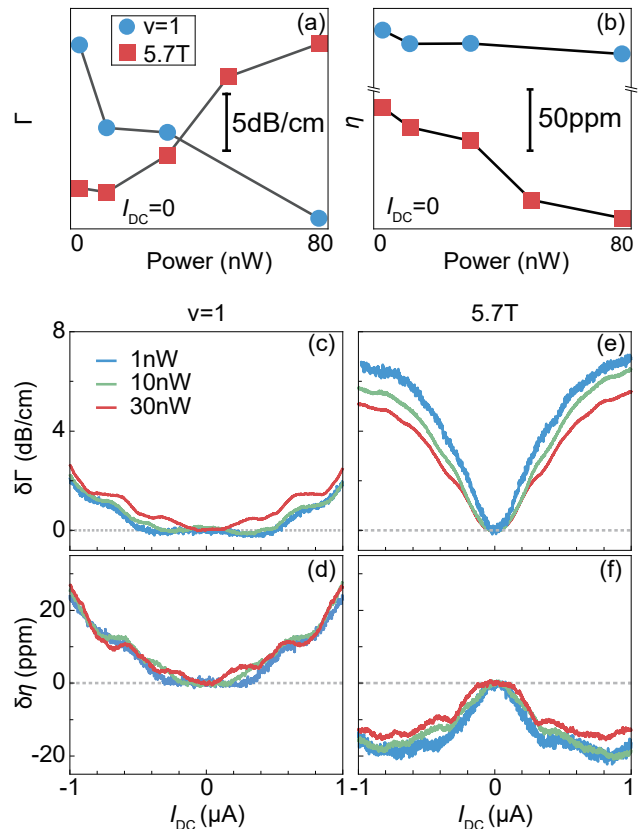


FIG. 4. (a-b) The variation of  $\Gamma$  and  $\eta$  with SAW power at zero  $I_{DC}$ . (c-f) The current-induced SAW attenuation variation  $\delta\Gamma$  and velocity shift  $\delta\eta$  at  $\nu = 1$  (left column) and  $B = 5.7$  T (right column), using different probing SAW powers.

No. 2021ZD0302602) for sample fabrication and measurement.

\* liuyang02@pku.edu.cn

† xilin@pku.edu.cn

- [1] K. v. Klitzing, G. Dorda, and M. Pepper, Phys.Rev.Lett. **45**, 494 (1980).
- [2] H. A. Tsui, D.C.and Stormer, Phys.Rev.Lett. **48**, 1559 (1982).
- [3] J. K.Jain, CompositeFermion (Cambridge University Press, 2007) pp. 1–11.
- [4] R. E. Prange, S. M. Girvin, et al., The Quantum Hall Effect [electronic resource] (New York, NY: Springer US, 1989) pp. 1–35.
- [5] E. Wigner, Phys. Rev. **46**, 1002 (1934).
- [6] Y. E. Lozovik and V. Yudson, ZhETF Pisma Redaktsiui **22**, 26 (1975).
- [7] P. K. Lam and S. M. Girvin, Phys. Rev. B **30**, 473 (1984).
- [8] D. Levesque, J. J. Weis, and A. H. MacDonald, Phys. Rev. B **30**, 1056 (1984).



- [9] R. L. Willett, H. L. Stormer, D. C. Tsui, L. N. Pfeiffer, K. W. West, and K. W. Baldwin, *Phys. Rev. B* **38**, 7881 (1988).
- [10] X. Zhu and S. G. Louie, *Phys. Rev. B* **52**, 5863 (1995).
- [11] A. A. Koulikov, M. M. Fogler, and B. I. Shklovskii, *Phys. Rev. Lett.* **76**, 499 (1996).
- [12] R. Du, D. Tsui, H. Stormer, L. Pfeiffer, K. Baldwin, and K. West, *Solid State Communications* **109**, 389 (1999).
- [13] M. P. Lilly, K. B. Cooper, J. P. Eisenstein, L. N. Pfeiffer, and K. W. West, *Phys. Rev. Lett.* **82**, 394 (1999).
- [14] L. W. Engel, D. Shahar, i. m. c. Kurdak, and D. C. Tsui, *Phys. Rev. Lett.* **71**, 2638 (1993).
- [15] Y. Chen, R. M. Lewis, L. W. Engel, D. C. Tsui, P. D. Ye, L. N. Pfeiffer, and K. W. West, *Phys. Rev. Lett.* **91**, 016801 (2003).
- [16] R. M. Lewis, Y. P. Chen, L. W. Engel, D. C. Tsui, L. N. Pfeiffer, and K. W. West, *Phys. Rev. B* **71**, 081301 (2005).
- [17] H. Zhu, G. Sambandamurthy, Y. P. Chen, P. Jiang, L. W. Engel, D. C. Tsui, L. N. Pfeiffer, and K. W. West, *Phys. Rev. Lett.* **104**, 226801 (2010).
- [18] A. Hatke, Y. Liu, L. Engel, M. Shayegan, L. Pfeiffer, K. West, and K. Baldwin, *Nature communications* **6**, 7071 (2015).
- [19] A. T. Hatke, Y. Liu, L. W. Engel, L. N. Pfeiffer, K. W. West, K. W. Baldwin, and M. Shayegan, *Phys. Rev. B* **95**, 045417 (2017).
- [20] A. Wixforth, J. P. Kotthaus, and G. Weimann, *Phys. Rev. Lett.* **56**, 2104 (1986).
- [21] A. Wixforth, J. Scriba, M. Wassermeier, J. P. Kotthaus, G. Weimann, and W. Schlapp, *Phys. Rev. B* **40**, 7874 (1989).
- [22] R. L. Willett, M. A. Paalanen, R. R. Ruel, K. W. West, L. N. Pfeiffer, and D. J. Bishop, *Phys. Rev. Lett.* **65**, 112 (1990).
- [23] M. A. Paalanen, R. L. Willett, P. B. Littlewood, R. R. Ruel, K. W. West, L. N. Pfeiffer, and D. J. Bishop, *Phys. Rev. B* **45**, 11342 (1992).
- [24] R. L. Willett, R. R. Ruel, K. W. West, and L. N. Pfeiffer, *Phys. Rev. Lett.* **71**, 3846 (1993).
- [25] R. L. Willett, K. W. West, and L. N. Pfeiffer, *Phys. Rev. Lett.* **88**, 066801 (2002).
- [26] B. Friess, Y. Peng, B. Rosenow, F. von Oppen, V. Umansky, K. von Klitzing, and J. H. Smet, *Nature Physics* **13**, 1124 (2017).
- [27] B. Friess, V. Umansky, K. von Klitzing, and J. H. Smet, *Phys. Rev. Lett.* **120**, 137603 (2018).
- [28] B. Friess, I. A. Dmitriev, V. Umansky, L. Pfeiffer, K. West, K. von Klitzing, and J. H. Smet, *Phys. Rev. Lett.* **124**, 117601 (2020).
- [29] I. L. Drichko, I. Y. Smirnov, A. V. Suslov, and D. R. Leadley, *Phys. Rev. B* **83**, 235318 (2011).
- [30] I. L. Drichko, I. Y. Smirnov, A. V. Suslov, L. N. Pfeiffer, K. W. West, and Y. M. Galperin, *Phys. Rev. B* **92**, 205313 (2015).
- [31] I. Drichko, I. Y. Smirnov, A. Suslov, Y. Galperin, L. Pfeiffer, and K. West, *Low Temperature Physics* **43**, 86 (2017).
- [32] M. Wu, X. Liu, R. Wang, Y. J. Chung, A. Gupta, K. W. Baldwin, L. Pfeiffer, X. Lin, and Y. Liu, *Phys. Rev. Lett.* **132**, 076501 (2024).
- [33] T. Arikawa, K. Hyodo, Y. Kadoya, and K. Tanaka, *Nature Physics* **13**, 688 (2017).
- [34] R. J. Haug, K. v. Klitzing, R. J. Nicholas, J. C. Maan, and G. Weimann, *Phys. Rev. B* **36**, 4528 (1987).
- [35] R. G. Clark, S. R. Haynes, A. M. Suckling, J. R. Mallett, P. A. Wright, J. J. Harris, and C. T. Foxon, *Phys. Rev. Lett.* **62**, 1536 (1989).
- [36] L. W. Engel, S. W. Hwang, T. Sajoto, D. C. Tsui, and M. Shayegan, *Phys. Rev. B* **45**, 3418 (1992).
- [37] R. R. Du, A. S. Yeh, H. L. Stormer, D. C. Tsui, L. N. Pfeiffer, and K. W. West, *Phys. Rev. Lett.* **75**, 3926 (1995).
- [38] P. Wang, J. Sun, H. Fu, Y. Wu, H. Chen, L. N. Pfeiffer, K. W. West, X. C. Xie, and X. Lin, *Phys. Rev. Res.* **2**, 022056 (2020).
- [39] X. Wang, H. Fu, L. Du, X. Liu, P. Wang, L. N. Pfeiffer, K. W. West, R.-R. Du, and X. Lin, *Phys. Rev. B* **91**, 115301 (2015).
- [40] J. Sun, J. Niu, Y. Li, Y. Liu, L. Pfeiffer, K. West, P. Wang, and X. Lin, *Fundamental Research* **2**, 178 (2022).
- [41] N. Samkharadze, K. A. Schreiber, G. C. Gardner, M. J. Manfra, E. Fradkin, and G. A. Csáthy, *Nature Physics* **12**, 191 (2016).
- [42] K. A. Schreiber, N. Samkharadze, G. C. Gardner, Y. Lyanda-Geller, M. J. Manfra, L. N. Pfeiffer, K. W. West, and G. A. Csáthy, *Nature Communications* **9**, 2400 (2018).
- [43] K. Huang, P. Wang, L. N. Pfeiffer, K. W. West, K. W. Baldwin, Y. Liu, and X. Lin, *Phys. Rev. Lett.* **123**, 206602 (2019).
- [44] A. Hutson and D. L. White, *Journal of Applied Physics* **33**, 40 (1962).
- [45] P. Bierbaum, *Applied Physics Letters* **21**, 595 (1972).
- [46] M. Wu, X. Liu, R. Wang, X. Lin, and Y. Liu, *arXiv:2311.01718 [physics.app-ph]* (2024).
- [47] L. Zhao, W. Lin, Y. J. Chung, K. W. Baldwin, L. N. Pfeiffer, and Y. Liu, *Chinese Physics Letters* **39**, 97301 (2022).
- [48] Recently, Wu et al.[32] revealed an interesting discovery: a noticeable modulation in the SAW velocity appears when varying current through the 2DES.